INTERNATIONAL JOURNAL FOR NUMERICAL AND ANALYTICAL METHODS IN GEOMECHANICS, VOL. 20, 155–171 (1996)

EXPERIMENTAL AND NUMERICAL SIMULATION OF SOLUTE TRANSPORT IN HETEROGENEOUS POROUS MEDIA*

A. BOUHROUM AND M. BAI

School of Petroleum and Geological Engineering, The University of Oklahoma, 100E. Boyd Street, Energy Center, T301, Norman, OK 73019, USA

SUMMARY

The effect of heterogeneity on solute transport in porous media is examined by means of physical experiments and controlled numerical simulations. The special cases of layered, clogged and aggregated porous media are particularly investigated. The breakthrough curves (BTCs) obtained from some sections of the physical models are extremely distorted with extended concentration tails. These tailings are caused by different trajectories of the tracer through fine (millimeter and centimeter) scale spatial heterogeneities. On the other hand, BTCs in sections of the physical models having no heterogeneous nature, showed classical 'S'-shape.

A computer simulation based on an improved capacitance model[1] was used to match the experimental data. The BTCs can be represented adequately by the model. However, it seems necessary to determine the fitting parameters experimentally in order to relate them to actual physical phenomena.

KEY WORDS: pollutant migration; solute breakthrough curves; numerical simulation; porous media

INTRODUCTION

The prediction of pollutant migration is one of the most important procedures in current environmental issues. Extensive interest has been demonstrated in the study of physical non-equilibrium status of solute breakthrough curves observed frequently in experimental tests. Recently, researchers began to recognize that spatial variation in porous media permeability strongly influences the time-dependency or non-fickian behaviour of solute dispersion. It is understood that the existence of heterogeneities at various scales limits the use of the classical convection–dispersion approach because, the transport process is not a combination of statistical sequences with normal distribution, and thus is a non-Gaussian nature.

Various models describing tailed breakthrough curves have been formulated.[2–4] In the capacitance approach, interacting media are considered to consist of regions of micropores and macropores. Micropores are assumed to be occupied by a stagnant fluid. Mass transfer between the flowing and the stagnant fluids is assumed to vary exponentially with time.[5] However, Bai *et al.*[1] pointed out that it is unreasonable to expect macropore type flow to occur in micropore, since the micropore region (matrix) is characterized by a low permeability. Therefore, the velocity field in micropores needs to be considered in transporting fluids and tracers. This assumption was validated experimentally by Bouhroum,[5] who showed that under relatively low flow velocity, the

* Dedicated to Professor Dagobert Kessel on the occasion of his 60th birthday

CCC 0363–9061/96/030155–17

Received February 1995
Revised 27 July 1995

local convective flow may be readily formed within the micropores. Furthermore, his experimental results using unconsolidated porous media suggested that the state of physical non-equilibrium due to finite size effect (i.e. permeability contrast) in heterogeneous porous media is primarily convective. The convection dominated transport was also supported by Mckibbin[6] who suggested that the onset of fluid convection for layered media was attributed to permeability contrast between layers. Further support of the convective model has also been provided by past experimental results which indicated that the long tails in the breakthrough curves are the result of structural change in porous media induced by particle clogging.[7] The blockage of pore necks through migrating particulate in the well connected porous media tends to create higher velocity in preferential flow pathways and thus leads to early solute penetration. The existence of low permeability zones delays the rate of solute transport and increases the skewness of the breakthrough curves. As an extension of the previous work by Bai *et al.*,[1] the current investigation focuses on the effect of different kinds of heterogeneities on tracer dispersion and on the comparative study between the model predictions and the experimental results. Detailed analysis of the significance of the local variations of fluid velocities generated by permeability variance on the scale dependence of the state of physical non-equilibrium is outlined. Besides the deterministic pore space heterogeneities (stratified porous media), broad distribution of pore sizes (aggregated porous media), and randomly clogged porous media are used to emphasize the practical significance of the convective effect in terms of interpretation of BTCs.

GOVERNING EQUATIONS

Assuming a constant flow through the porous media, the convective model proposed by Bai *et al.*[1] can be given in the following form:

$$D_1 \frac{\partial^2 c_1}{\partial x^2} - v \frac{\partial c_1}{\partial x} = f \frac{\partial c_1}{\partial t} + K(c_1 - c_2) \tag{1}$$

$$-\frac{v}{b} \frac{\partial c_2}{\partial x} = (1 - f) \frac{\partial c_2}{\partial t} - K(c_1 - c_2) \tag{2}$$

where c_1 and c_2 are the solute concentrations for macro- and micropores, respectively; D_1 is the macropore dispersion coefficient, v is the average interstitial velocity, b is the inverse of velocity factor, f is the fraction of fluid in macropores, K is the rate of mass transport between micro- and macropores, x is the distance from source, and t is the time.

For more general solution, the following dimensionless terms are defined:

$$y = \frac{x}{L}, \qquad \tau = \frac{vt}{L}, \qquad a = \frac{KL}{v}, \qquad \gamma = \frac{vL}{D_1} \tag{3}$$

where L is the length of a laboratory sample column, or the longest traveling distance of solute; y is the dimensionless distance, τ is the dimensionless time or pore volume injected, γ is the equivalent Peclet number indexing the ratio of the transport rates by convection to that by dispersion, a is the rate coefficient of internal flow.

With the substitution of the dimensionless terms, equations (1) and (2) can be rewritten as

$$\frac{1}{\gamma} \frac{\partial^2 c_1}{\partial y^2} - \frac{\partial c_1}{\partial y} = f \frac{\partial c_1}{\partial \tau} + a(c_1 - c_2) \tag{4}$$

$$-\frac{1}{b} \frac{\partial c_2}{\partial y} = (1 - f) \frac{\partial c_2}{\partial \tau} - a(c_1 - c_2) \tag{5}$$

Equations (4) and (5) represent the dimensionless form of the governing equations of solute transport in heterogeneous porous media incorporating micropore convection. Analytical solutions were obtained from the coupled equations (4) and (5) using the method of differential operator. Detailed solutions and their procedure are given elsewhere (Reference 1).

EXPERIMENTAL METHODS

Miscible displacement experiments were performed with NaCl–water solution (0·25 $g l^{-1}$) — with a viscosity ratio of 1·0 and a density contrast of 1×10^{-4} $g l^{-1}$ so that no viscosity or density instabilities are induced — through distilled water saturated heterogeneous porous media. The experiments were performed on two parallepepedic prototypes. The sample had internal dimensions of 120 cm in length, 12 cm in width and 1 cm in height for the layered and aggregated porous media. For the clogged porous media the dimensions were 40 cm × 20 cm × 2 cm, respectively. The prototypes were made of plexiglas to observe the progress of particulates migration as well as a companion dye tracer injected simultaneously with NaCl. The *in situ* conductivity measurement technique[8] with a set of fourty eight flow-through conductivity detectors that provide time variation of concentration at 16 cross sections of different distances from the cell's inlet was used (see Figure 1). The following pore space and flow heterogeneities were investigated.

Stratified porous media

The case of layered porous media is of interest because it corresponds to large-scale variations of the petrophysical properties such as porosity and permeability. Moreover, this type of heterogeneity has two well defined length scales: layer thickness and grain size. The effects of layer orientation and the number of layers on breakthrough curves have been studied. The samples consisted of alternating layers of glass beads. The permeability ratio between the three strata varied in a range of 1:7·40:13·27 and the layers were parallel to the flow.

Aggregated porous media

This type of heterogeneities corresponds to small-scale variations in petrophysical properties encountered in sand packings, laboratory cores, and fractured porous media with a large range of apertures. These porous media are characterized by strong velocity differences between neighboring channels leading to preferential flow processes. The larger flow velocity inside these preferred flow paths exerts a dominating influence on the characteristic transport time. The aggregated heterogeneity was fabricated from a mixture of coarse-grained (400 μm), medium-grained (150 μm) and fine-grained (90 μm) sand.

Randomly clogged porous media

Typical examples of clogged porous media occur in percolation process in a homogeneous porous media where the connectivity of the medium diminishes as a result of the blockage of pores. Another example of clogged porous media occurs during fines migration in porous media where the pore blockage is a result of the interaction of the particles with the pores by size and hydrodynamic exclusion processes. Damaged formations, damaged gravel-packs, and deep bed filters are the examples of this kind of clogged porous media. The clogged porous media were made up from gradually migrating smaller glass beads front ($d_s = 400$ μm) through a second

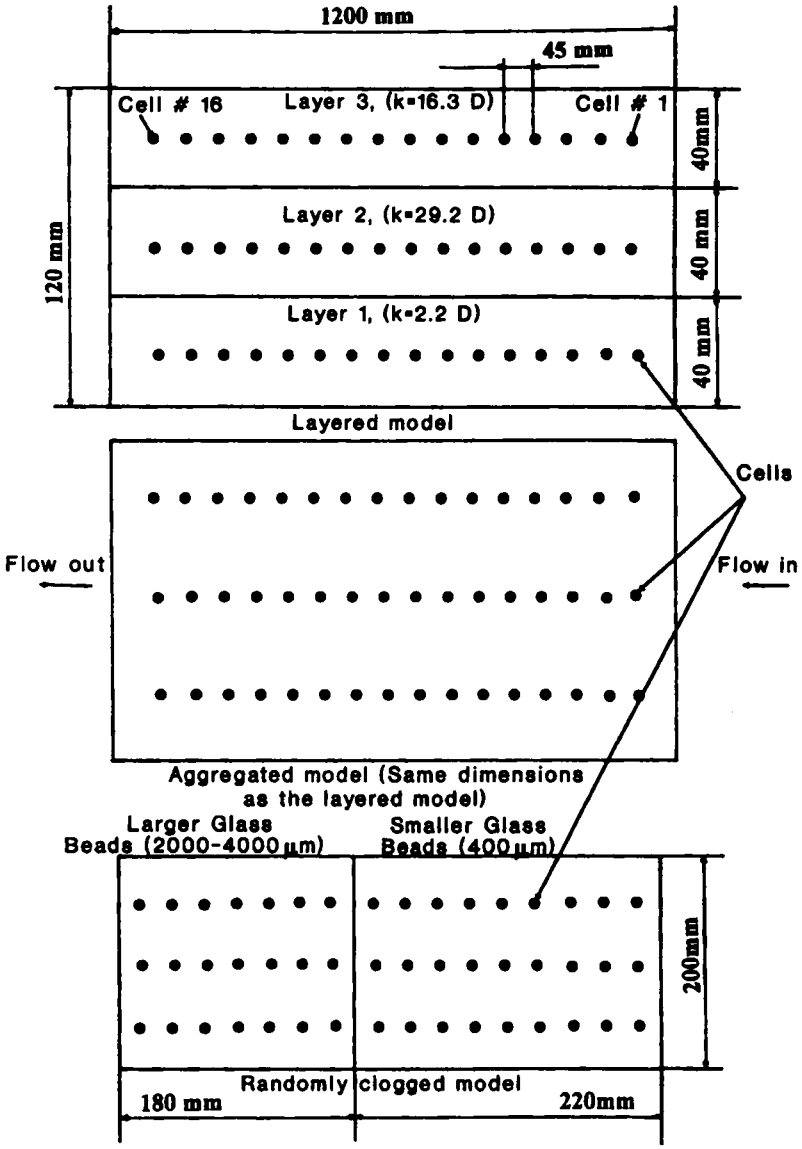

Figure 1. Dimensions and configurations of the used samples

layer of a mixture of larger glass beads (d_l = 2000–4000 µm), with incremental small particle migration into and through the larger mixture initiated by gradual increase of the flow rate up to 53 l h^{-1}.

EXPERIMENTAL RESULTS

Layered porous media

Figure 2 displays three types of BTCs obtained from a three-layer sample corresponding to the same flow rate but different permeability (D^* = Darcy). In the high permeability layer,

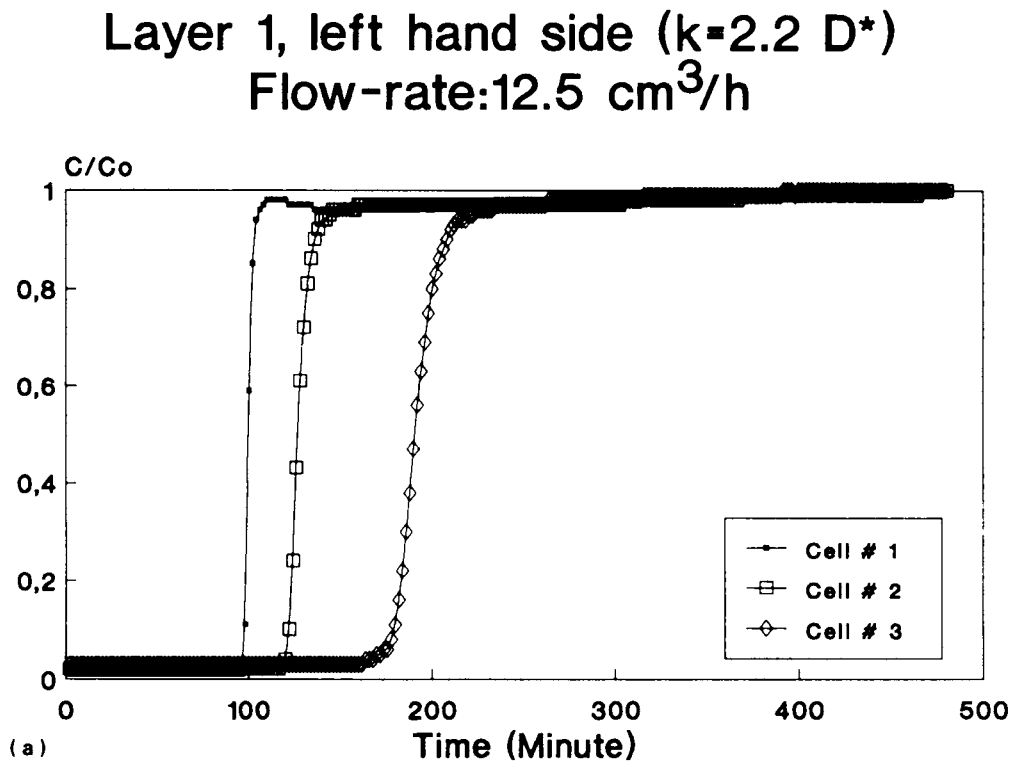

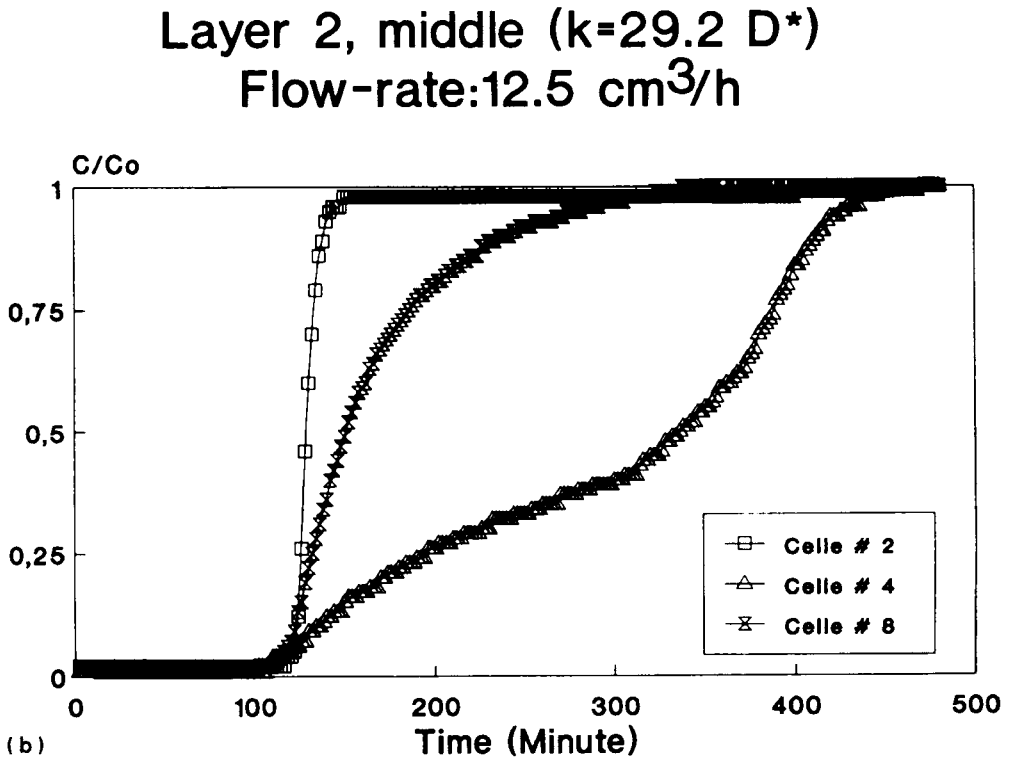

Figure 2. Experimental BTCs in a layered medium with three alternating layers of glass beads with high, medium and low permeability

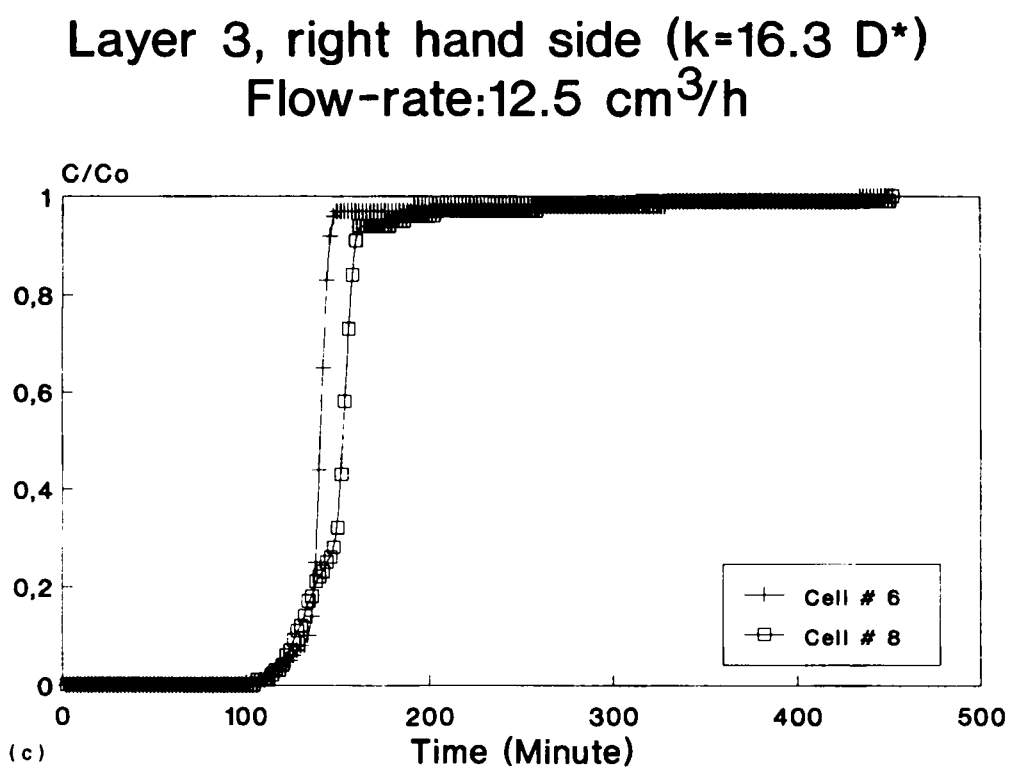

Figure 2. (Continued)

the BTC of cell No. 4 show a strong tail. Tracer transport is considerably delayed after a steep rise up to $C/C0 = 0{\cdot}50$. However, near the inlet of the prototype the BTC of cell No. 2 is "S"-shaped while the BTC of cell No. 8 shows two distinct inflection points indicating that the tracer moves separately at different velocities with considerable mixing between two types of layers as it is shown by the corresponding increase in the leading part of the BTC in the neighboring layer (see Figure 2(c)). In the left-hand side layer a reverse trend with a very early appearance of tracer is observed as experienced by BTC of cell No. 16 of Figure 3(c). The interlayer dispersion between the high and the low permeability layers is not strong enough to exert any effect on its BTCs, as shown in Figures 2(a) and 3(a). Mixing between layers with increasing permeability difference seems to have been much less dominated. The incomplete concentration mixing between layers is due to transverse dispersion which is not efficient enough to evenly sample these permeability differences.

Aggregated porous media

Breakthrough curves obtained at different sections of the prototype are presented in Figure 4. The BTCs of cells Nos. 1 and 8 in Figure 4(a), Nos. 1 and 8 in Figure 4(b) and Nos. 1 and 8 in Figure 4(c) exhibit a behaviour typical of solute transport in homogeneous porous media, while BTCs of cells Nos. 7, 2, 3 and 5 in Figure 4(a), (b) and (c), respectively, are much less symmetrical, wherein the BTCs show a strongly skewed concentration pattern typically associated with

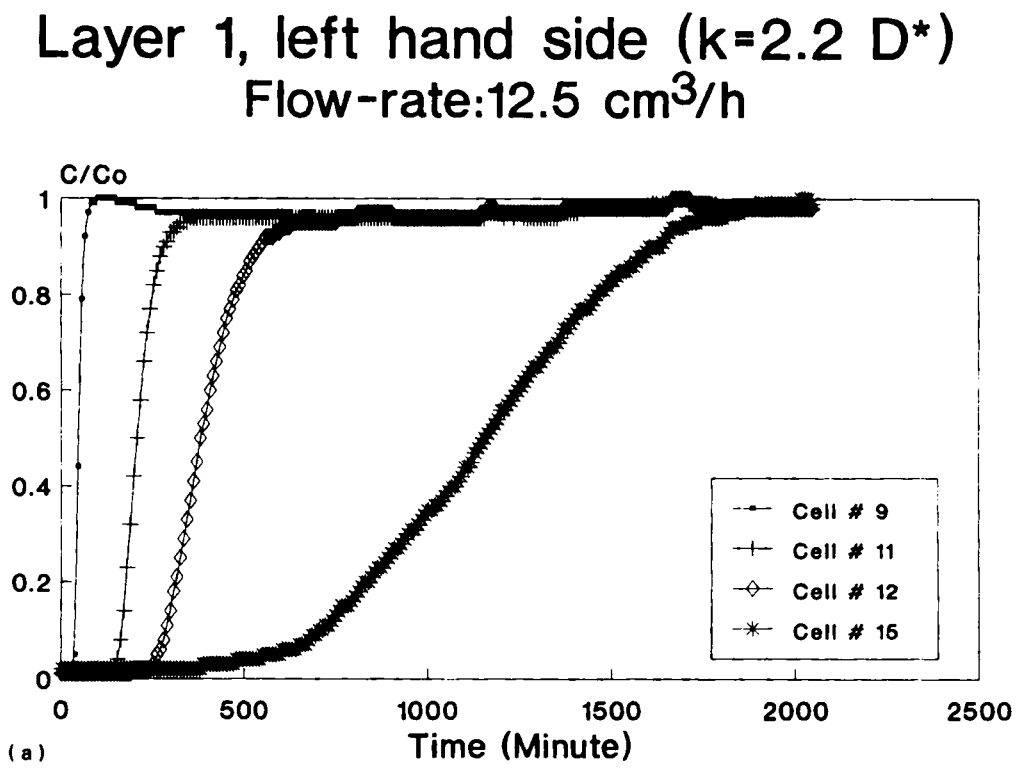

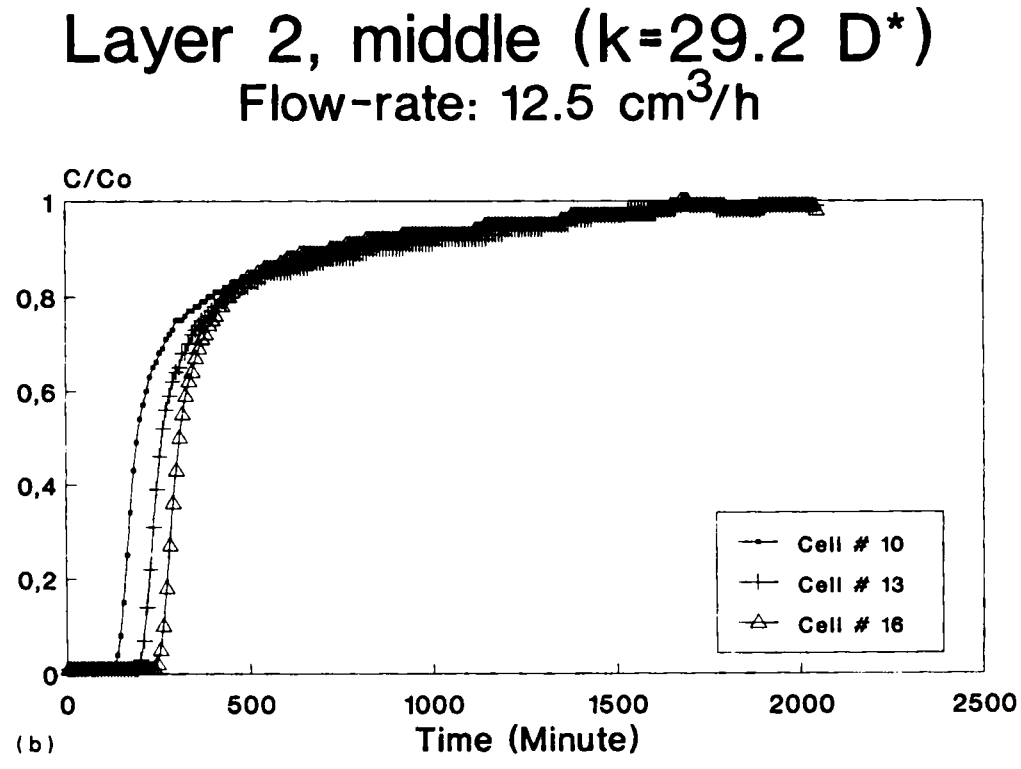

Figure 3. Experimental BTCs in a layered medium with three alternating layers of glass beads with high, medium and low permeability

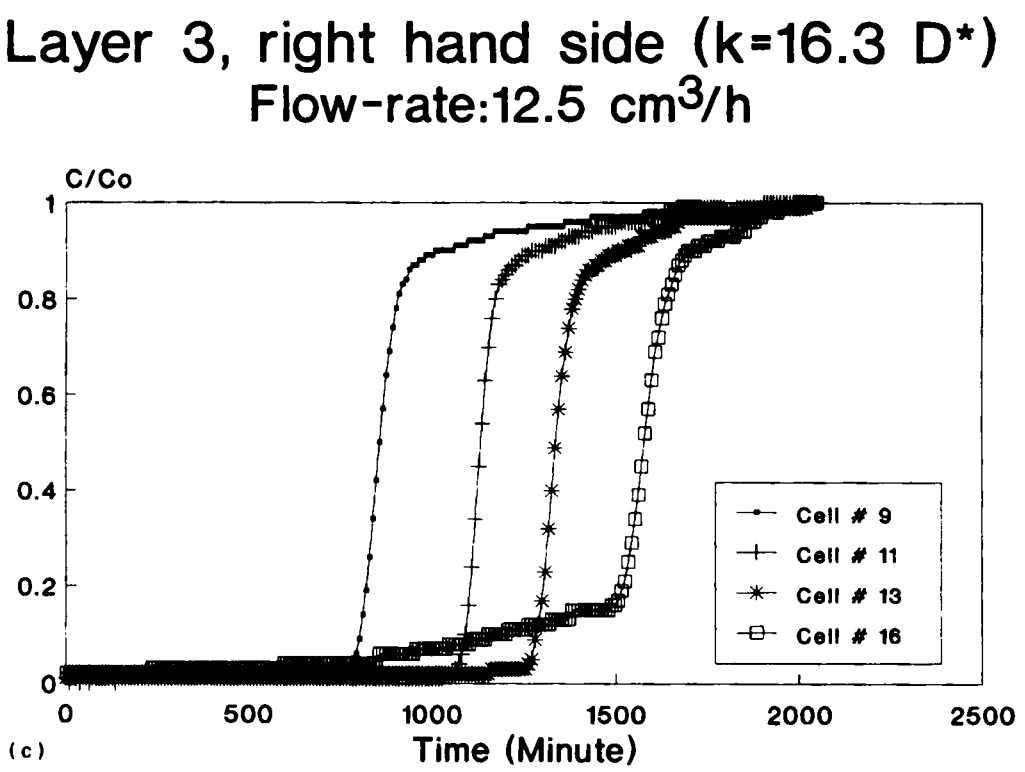

Figure 3. (Continued)

structured systems. This qualitative difference between the BTCs is clearly the result of small-scale heterogeneities. Such heterogeneities are due to different flow path formation with a broad flow velocity distribution. However, the compaction is believed to be of good quality and no channeling has been observed when using a dye tracer.

Randomly clogged porous media

Tracer BTCs obtained at different cross sections of the cell before any particulates migration are depicted in Figure 5(a). It can be seen that the BTCs are 'well behaved' and symmetrical. These features are characteristic of homogeneous porous media. The effect of clogging is shown in Figure 5(b). The BTCs are strikingly different from the previous ones with a pronounced tailing. There is much information available in each individual BTC as their shape difference reflects the sensivity of tracer dispersion to different flow heterogeneities and spatial velocity variation along the porous media. This additional spreading is indicative of preferential flow paths and dispersion into the low permeability zones. This further indicates that tracer particles are not flowing at a uniform average velocity as it is generally assumed. Thus the tracer particles dispersed into low permeability zone will tail behind those moving along the preferential flow paths. The general lack of symmetry in BTCs is a strong evidence that the blockage of pore necks through migrating particulates was significant.

It can be stated that the skewed BTCs are the result of delayed tracer particles that are attributed to spatial variability of permeability and not to the presence of any blind cavity or dead

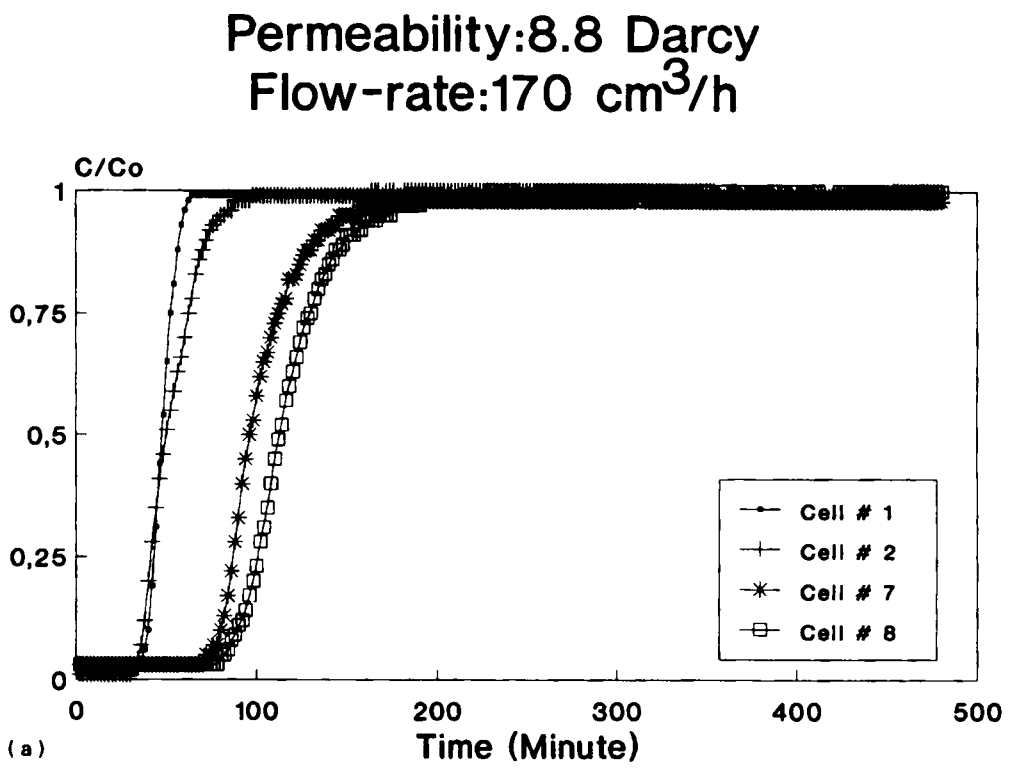

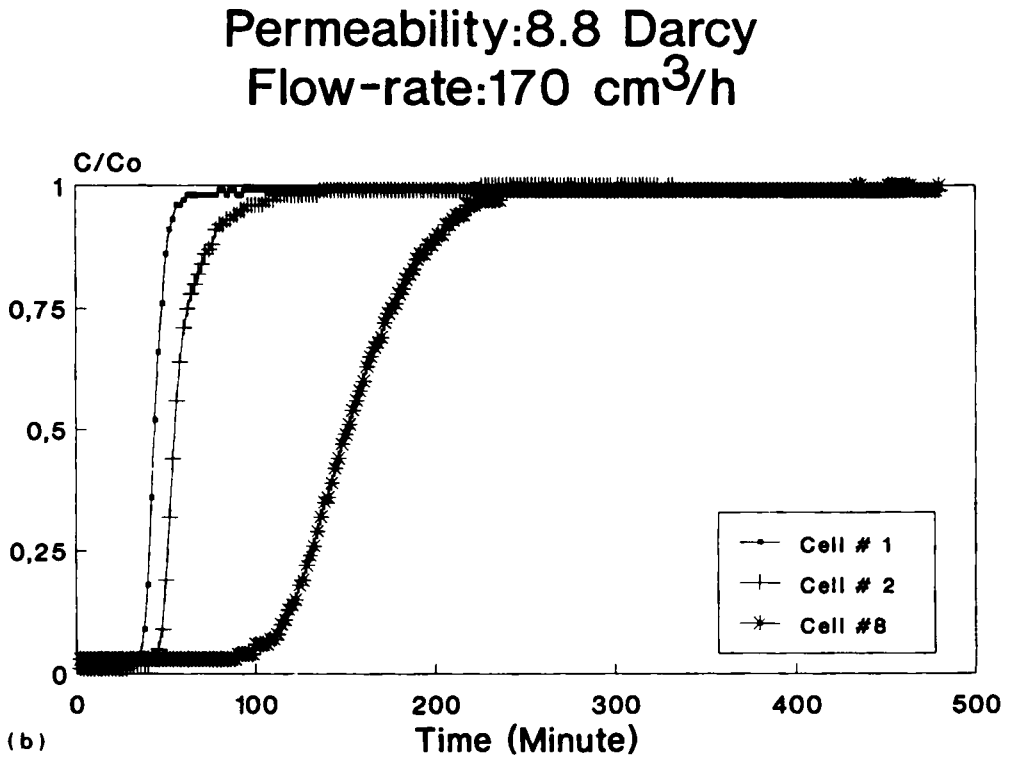

Figure 4. Experimental BTCs in an aggregated medium prepared from three sands of 90, 150 and 400 μm diameter for different sections

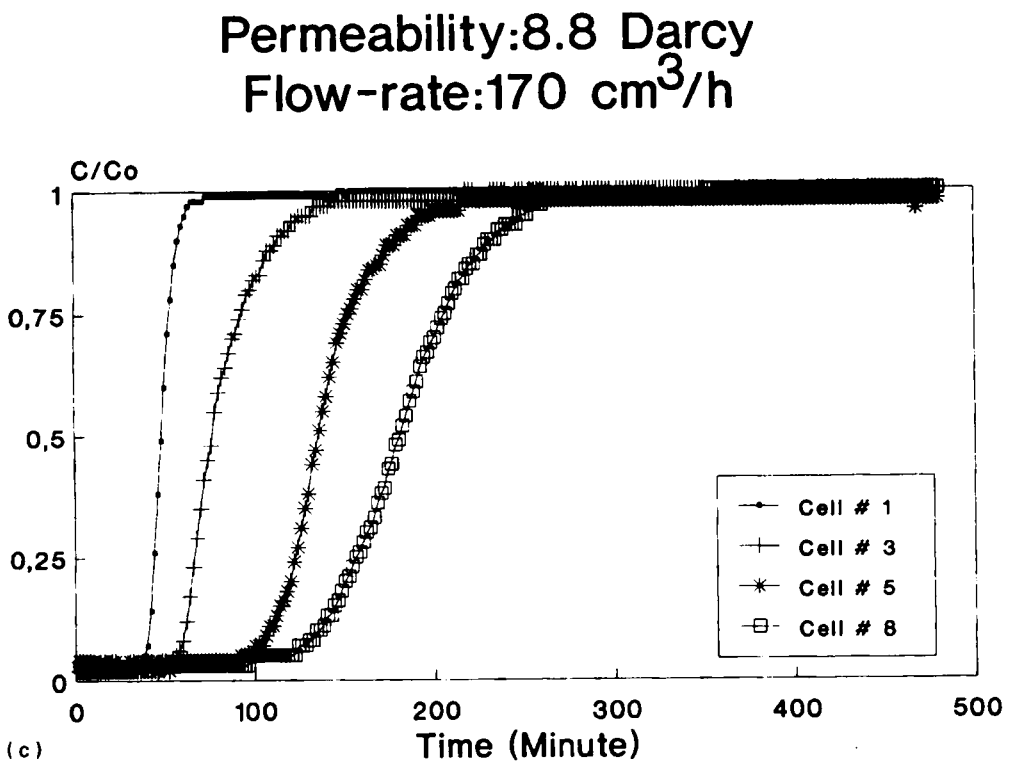

Figure 4. (Continued)

end pores. The occurrence of such isolated zones in the tested unconsolidated porous media, which are considered to be well connected, could not be observed. Therefore, the tailing of BTCs should disappear in samples with a large length compared to the heterogeneity size. A direct experimental support to this hypothesis is inferred from the BTCs measured after particulates breakthrough. The BTCs shown in Figure 6 are extremely flat, yet symmetrical. The breakthrough of particulates leads toward pore space homogenization. Therefore, the pore network of the clogged porous media has been unified and there is no preferential flow path. These results indicate that the tailing is not intrinsic to the system but is a finite size effect that disappears with the homogenization of the porous media.

MODEL APPLICATIONS

In the following the Bai *et al.* model[1] is applied to simulate some of the experimental BTCs obtained from three configurations of heterogeneous porous media. The model results are compared to the experimental BTCs by multi-parameter optimization. The fitting parameters and their magnitudes, dimensionless time and distance, together with the index in relation to individual figures are summarized in Table I.

Comparisons of the model simulation and the measured BTCs are presented in Figures 7–12 for various heterogeneous configurations investigated. All simulations of the layered and the aggregated porous media BTCs (Figures 7, 8, 10 and 12) closely predict the tailing and the initial part of the BTCs. The results consistently indicate that the improved capacitance model describes

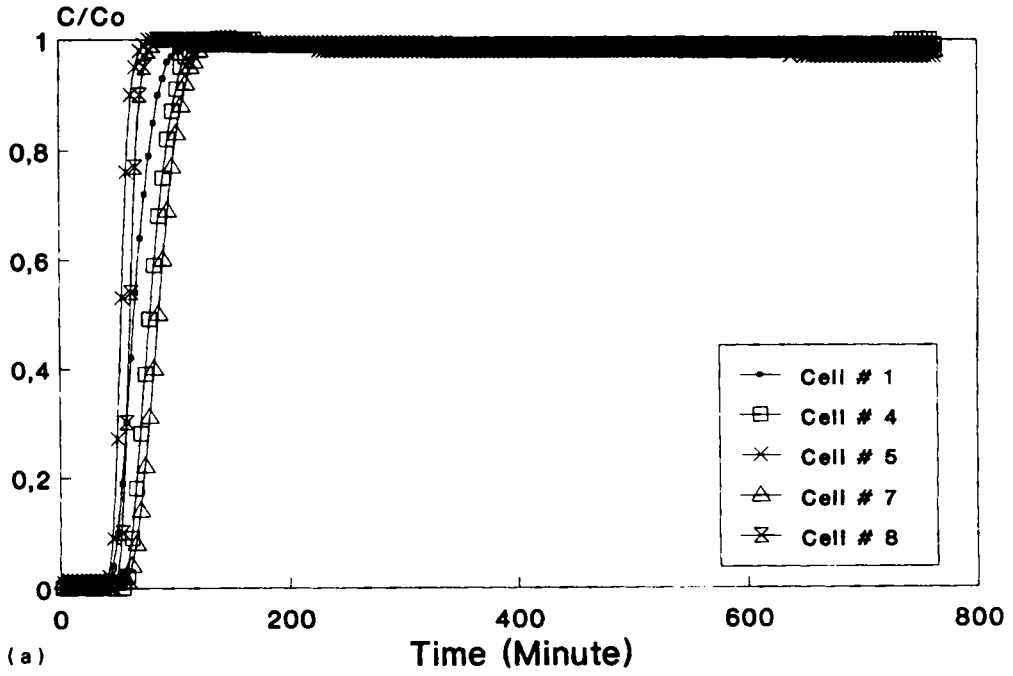

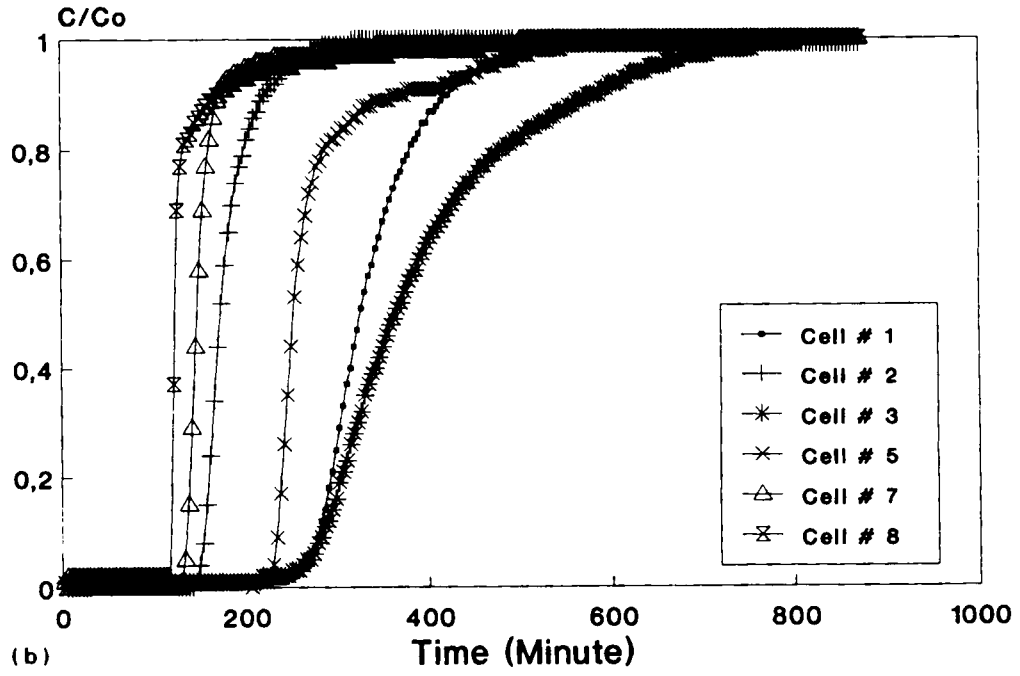

Figure 5. Experimental BTCs obtained before (a) and after (b) the clogging process due to particulates migration

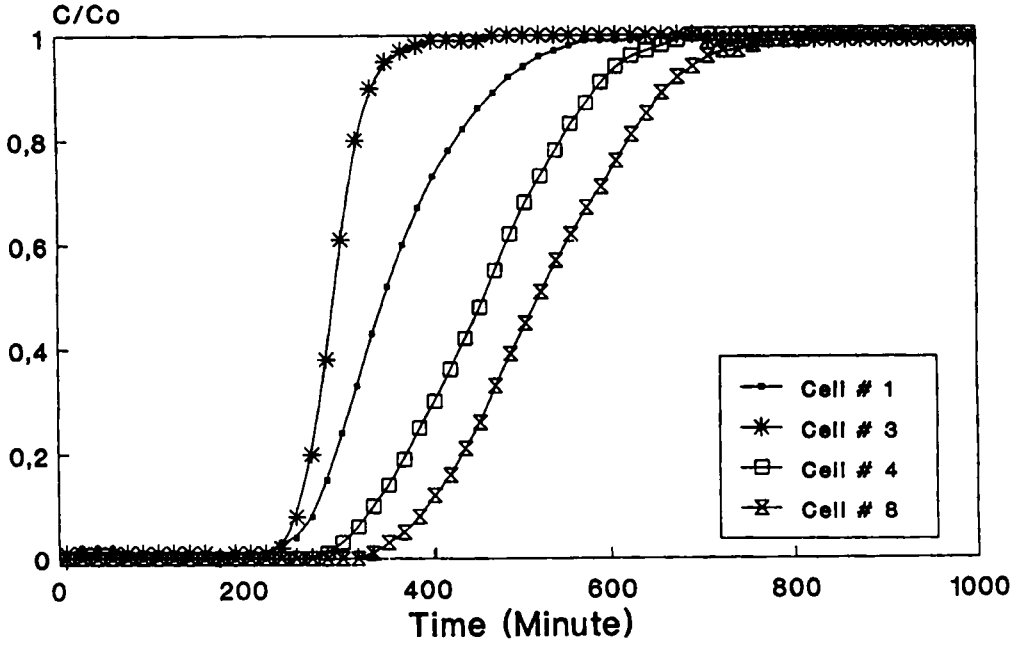

Figure 6. 'S'-shaped BTCs after pore space homogenization of the clogged porous media

Table I. Modeling parameters

Figure No.	γ	f	a	b	c_1	c_2	τ	y
7	18	0·74	0·59	0·8	1	0·7	1·3	0·65
8	10	0·98	0·34	1	1	0·1	0·5	0·1
9	10	0·95	0·38	1	1	0·1	0·5	0·1
10	10	0·97	0·36	1	1	0·1	0·5	0·1
11	15	0·86	0·50	0·85	1	0·8	1·1	0·55
12	10	0·93	0·39	0·95	1	0·3	0·6	0·17

the actual physical phenomena as these porous media are characterized by permeability variance but uniform active pores. The hypothesis of convective transport throughout the porous media is therefore validated. In the case of randomly clogged porous media, however, the fittings are not consistent. From Figure 9 it can be seen that the simulated curve overestimates the tailing. The reason for this discrepancy between model prediction and measurement is probably related to the peculiar shape of this BTC (Cell No. 5) when compared to BTCs in Figure 5(b). Indeed, the BTCs Nos. 1 and 5, which have different natures of the BTCs up to a concentration magnitude of about $C/C_0 = 0{\cdot}9$, become similar in shape in the latter part of the tailed region; it is inferred that the tracer particle velocity was identical, and that further structural changes in porous media occurred during the tracer injection. All the simulations produced with the improved model provide an excellent fit to the initial part of the BTCs. However, the improved model is capable of better predicting steep rising limbs of the BTCs when compared with flat rising limbs (see Figures 11 and 12) for the clogged porous media. This suggests that some pores become inactive in flow and transport due to a total blockage of the pores. This pore blockage induced heterogeneity has the size of few grains as shown by autoradiographed slice of the samples as shown elsewhere.[8]

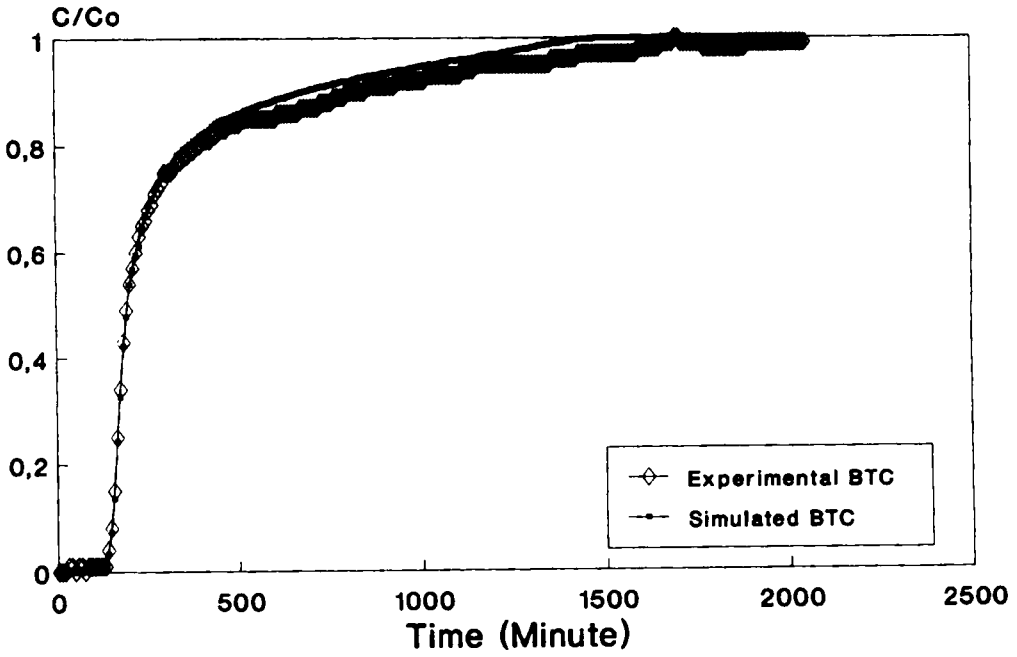

Figure 7. Comparison of experimental and simulated BTCs (Cell No. 10 from Figure 3(b)) produced with the improved capacitance model

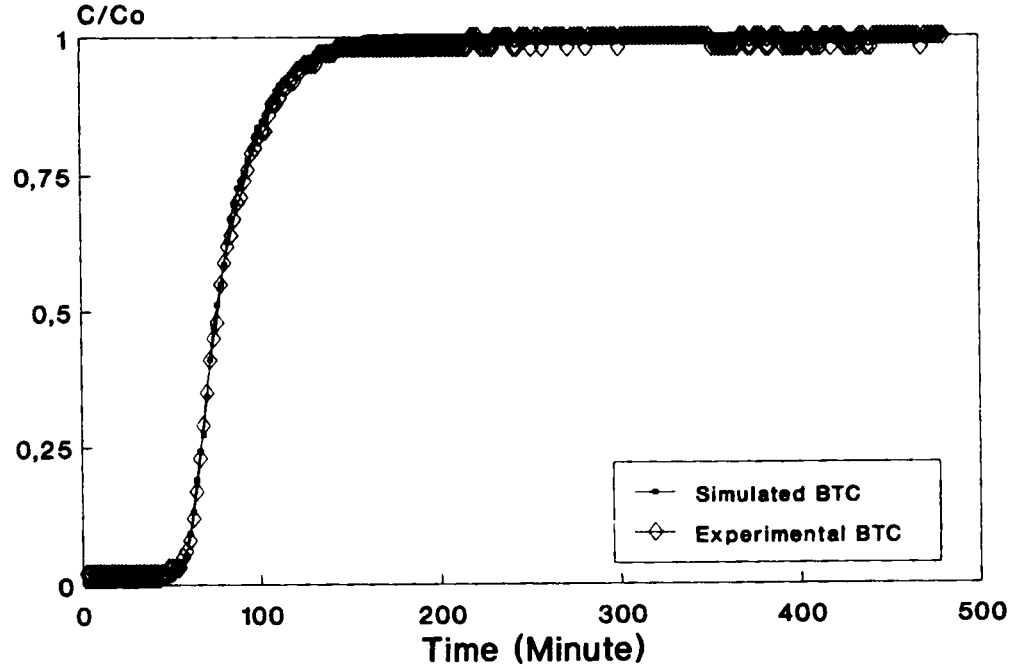

Figure 8. Comparison of experimental and simulated BTCs (Cell No. 3 from Figure 4(c)) produced with the improved capacitance model

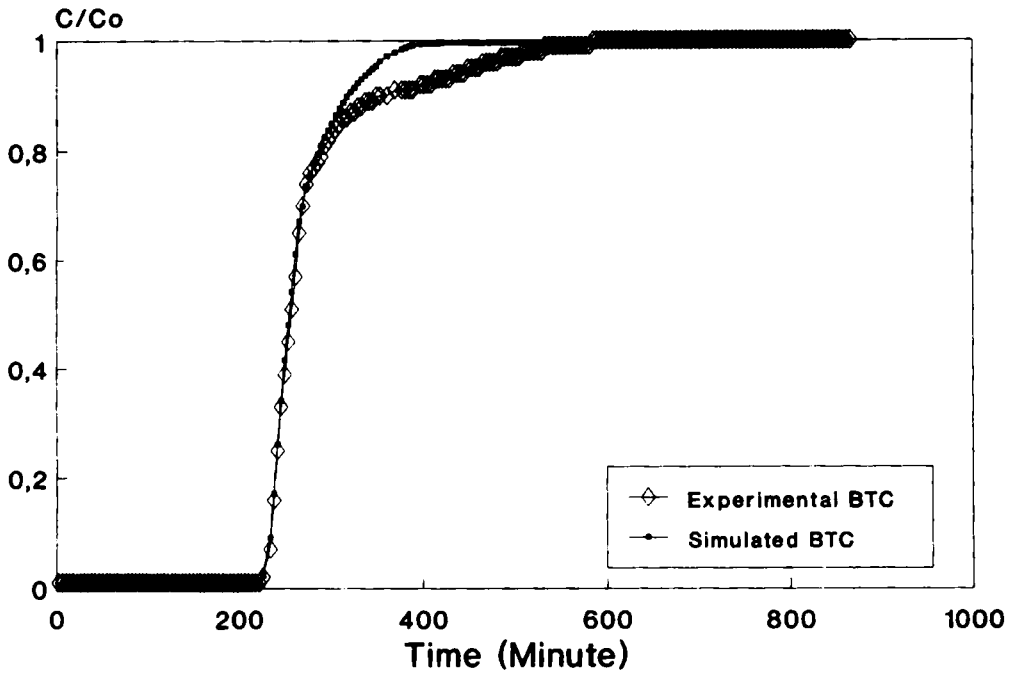

Figure 9. Comparison of experimental and simulated BTCs (Cell No. 5 from Figure 5(b)) produced with the improved capacitance model

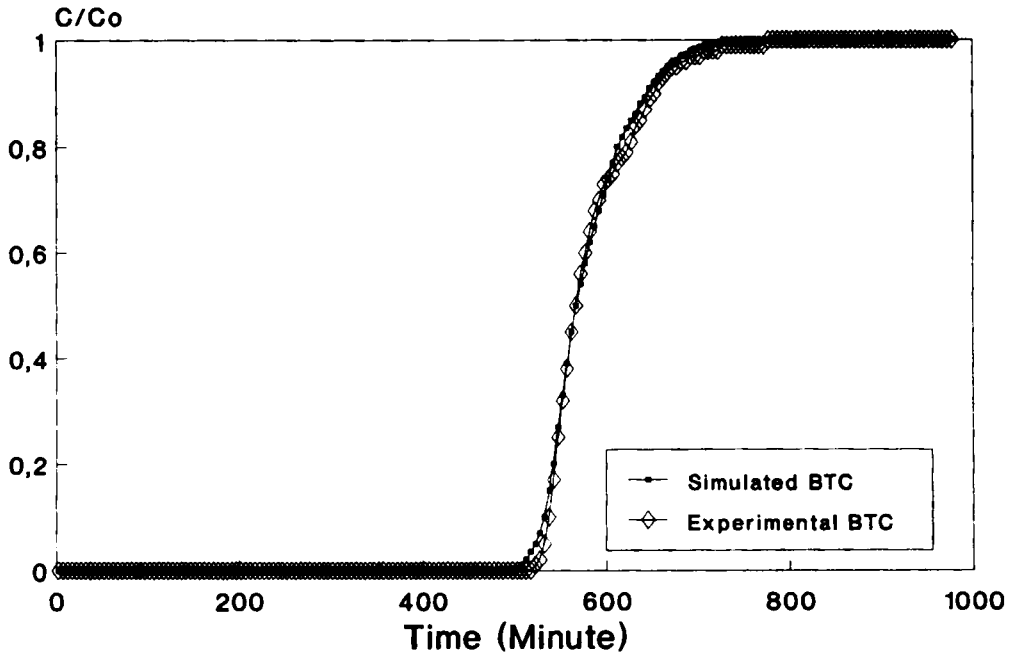

Figure 10. Comparison of experimental and simulated BTCs (Cell No. 7 from Figure 4(a)) in the aggregated porous media produced with the improved capacitance model

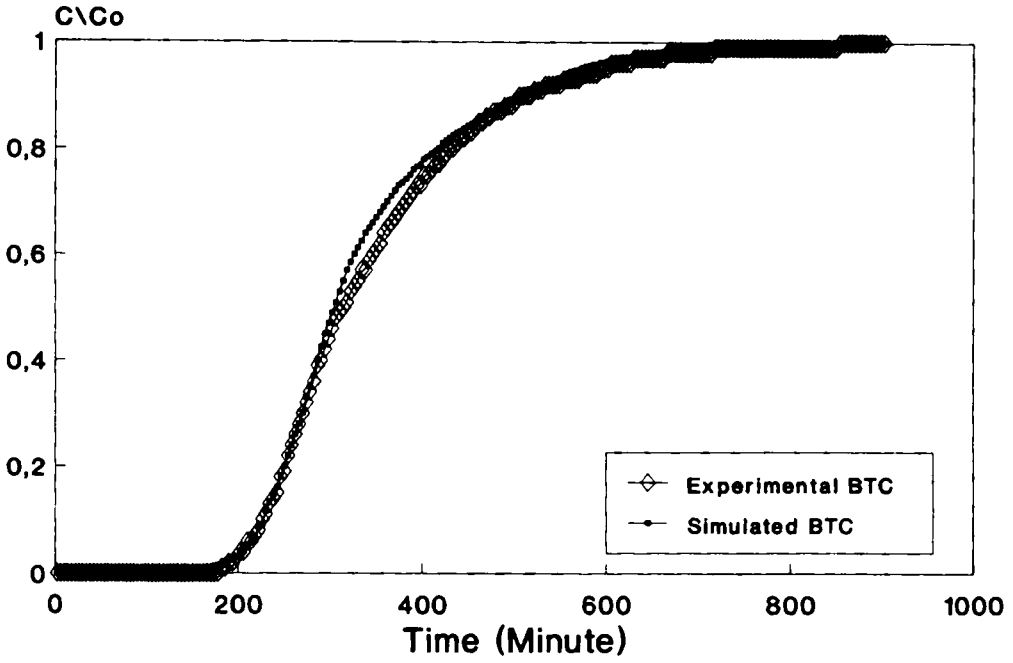

Figure 11. Comparison of experimental and simulated BTCs in clogged porous media (Cell No. 3 from Figure 5(b)) produced with the improved capacitance model

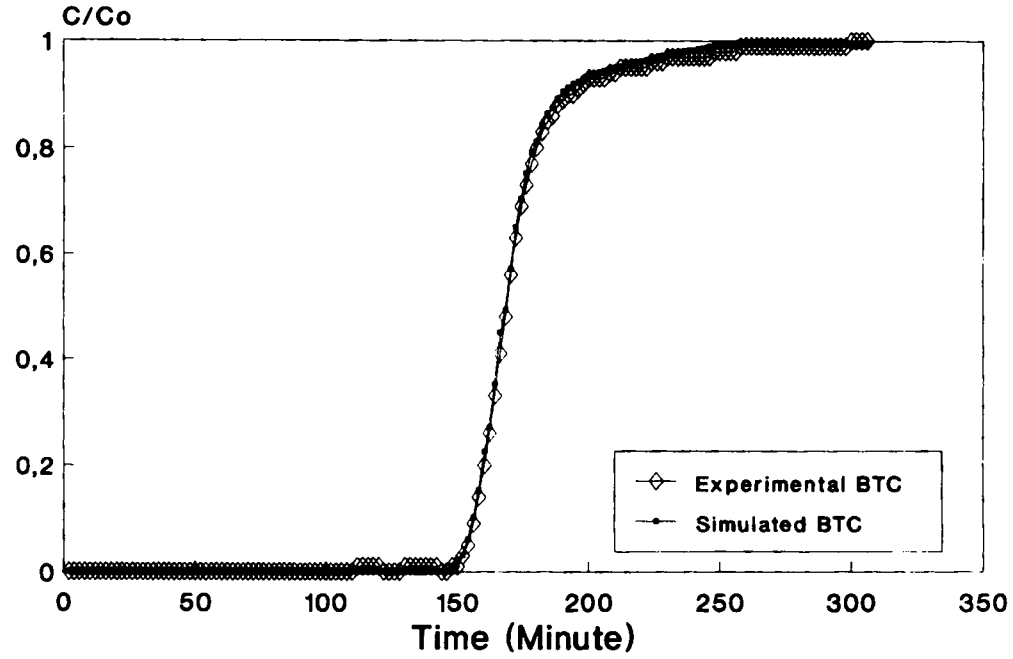

Figure 12. Comparison of experimental and simulated BTCs (Cell No. 2 from Figure 5(b)) in clogged porous medium produced with the improved capacitance model

This behaviour which is not expected in the improved model, which states that there are no blind cavities or dead end pores in the porous media, was violated through pores blockage. The pores become inactive so that the mobile-immobile concept used in the capacitance model would apply.

The analysis of the tracer dispersion data has revealed that, with some minor exceptions where the behaviour of pores change with time, the model can provide very good fits to the measured BTCs. This fitting process, however, also affects the values of the model parameters. Therefore, it is important to determine the parameters of the model independently and to compare them with values obtained by curve fittings.

CONCLUSIONS

Comparisons of the experimental results and model predictions have indicated that tailed BTCs are due to small and large scale heterogeneities in the pore structure caused by permeability variations. The BTCs demonstrate that individual tracer particles gradually sample the velocity fluctuations associated with the heterogeneity of porous media. Finite size effects were found to have a significant impact on the shape of the BTCs. However, these effects quickly disappear with the homogenization of the clogged porous media.

Simulations indicated that the model provides a valid tool to analyze the experimental data as long as the conceptualization of the flow system holds. The fitting process, however, affects the values of the additional parameters. Therefore, to analyse experimental data with higher degree of confidence the model parameters should be measured independently.

ACKNOWLEDGEMENTS

Support of the National Science Foundation under contract EEC-9209619 and support of the Alexander von Humboldt-Stiftung from Germany are gratefully acknowledged. M. Bai would also like to express his appreciation for Dr. J.-C. Roegiers for his support. The authors are thankful to the reviewers for their constructive comments and suggestions.

NOTATION

a	rate coefficient of internal flow
b	inverse of the intensity convection (velocity) factor
c_1	solute concentration for macropores
c_2	solute concentration for micropores
d_l	diameter of larger glass beads
d_s	diameter of smaller glass beads
D_l	macropore dispersion coefficient
f	fraction of fluid in macropores
K	rate of mass transport between micro- and macropores
L	length of a laboratory sample column, or the longest traveling distance of solute
t	time
v	average interstitial velocity
y	dimensionless distance
x	distance from source
γ	equivalent Peclet number indexing the ratio of the transport rates by convection to that by dispersion
τ	dimensionless time or pore volume injected

REFERENCES

1. M. Bai, A. Bouhroum, F. Civan and J.-C. Roegiers, 'Improved model for solute transport in heterogeneous porous media', *J. Petroleum Sci. Eng.* (in press).
2. K. H. Coats and B. D. Smith, 'Dead end pore volume and dispersion in porous media', *Society of Petroleum Engineers J.*, **4**, 73–84 (1964).
3. J. B. Passioura, 'Hydrodynamic dispersion in aggregated porous media. Parts I and II', *Soil Sci.*, **11**, 339–354 (1971).
4. M. L. Brusseau, R. E. Jessup and P. S. C. Rao, 'Modeling the transport of solutes influenced by multiprocess nonequilibrium', *Water Resour. Res.*, **25**, 1971–1988 (1989).
5. A. Bouhroum, 'Is Tailing of breakthrough curves diffusive? Theoretical and experimental evaluation', Proc. 5th Saskatchewan Petroleum Conference, Regina, Canada, October 18–20, 1993. Petroleum Society of CIM # 93-10-36.
6. R. McKibbin, 'Thermal convection in layered and anisotropic porous media. A review', Proc. CSRIO/DSIR Seminar on Convective Flows in Porous Media, Wellington, New Zealand, 1985, pp. 113–127.
7. A. Bouhroum, 'Einfluß von Nebenflußwegen auf die Verdrängung mischbarer Flüssigkeiten in porösen Medien', *Erdöl Erdgas Kohle Z.*, **108**, 22–29 (1992).
8. A. Bouhroum, 'Experimental study of dispersion in randomly clogged porous media', Proc. 45th annual Technical Meeting of the Petroleum Society of CIM, Calgary, Canada, June 12–15, 1994. Petroleum Society of CIM # 94-76.